3

Using Multi-temporal Satellite Images to Evaluate the Changes of Vegetation Index of Land Cover in Thai Binh Province

Pham Van Cu, Chu Xuan Huy, Nguyen Thi Thuy Hang, Rajesh Bahadur Thapa, Frédéric Borne

Satellite images highlight the existing situation and expected threats against environment. The integration of maps displaying vegetation and urban indices with statistic data on pig production allows us to make clear the relation between land cover changes and pig production development in Thai Binh.

Introduction

The spatial analysis introduced in this study contributes to identify the relationship between traditional agricultural practice and pig production activities at the provincial scale. Most of the studies carried out in the framework of our project used local statistic and cartographic data in accepting their heterogeneity in their reliability and their standards (see next chapters). Under this circumstance, the use of multi-temporal remotely sensed data will contribute to complete the lack of data in some cases and to provide another vision to understand the spatio-temporal evolution of the land cover in Thai Binh through a series of vegetation indices extracted from the images. The vegetation indices computed for the whole image are associated to communal administrative map of Thai Binh to create a time series of vegetation indices of each commune. The integration of maps displaying the vegetation indices with statistic data on pig production allows us to make clear the relation between land cover changes and pig production development in Thai Binh.

The current research aims to highlight the existing situation and expected threats against environment. This preliminary work will be the base for a decision making and strengthening tool for the Thai Binh's authorities in order to define urgently suitable technologies for land-use and investment planning, and to enforce the regulation considering environment. For this purpose, a series of multi-temporal satellite imageries are used to extract the vegetation index of the whole province for a period between 1975 up to 2003 in depending upon the availability of satellite images.

Material and methods

Used data

Satellite Images - Four Landsat images (1MSS, 1TM and 2 ETM+7 acquired respectively in November 1975, November 1989, September and November 2001) and three scenes of ASTER images (one in September 2002 and two in November 2003) were obtained for the study areas. The tables 1 and 2 present Landsat and ASTER data specifications respectively.

Ancillary data are supplied by administrative maps of Thai Binh and statistic yearbook on fertilizer consumption of Thai Binh

Table 1: Specification of Landsat data

Aquired in Dec. 1975 (Landsat MSS)			
Band number & wavelength (micro-meter)	**VNIR** (Visible & Near Infrared)	**SWIR** (Short Wave Infrared)	**TIR** (Thermal Infrared)
	Band 4 (Green): 0.50~0.60		
	Band 5 (Red): 0.6~0.7	*Band 7: 0.9~1.1*	
	Band 6: 0.7~0.9		
Spatial Resolution	*57m * 79m*	*57m * 79m*	*Nil*
Swath width	*185 km*		
Acquired in Nov. 1989 (Landsat TM) and Sep. 2001, Nov. 2001 (Landsat ETM+7)			
Band number & wavelength (micro-meter)	**VNIR** (Visible & Near Infrared)	**SWIR** (Short Wave Infrared)	**TIR** (Thermal Infrared)
	Band 1 (Blue): 0.45~0.52	*Band 5: 1.55~1.75*	
	Band 2 (Green): 0.52~0.6		
	Band 3 (Red): 0.63~ 0.69	*Band 7: 2.08~ 2.35*	*Band 6: 10.4~ 12.5*
	Band 4 (NIR): 0.76~ 0.9		
	Panchromatic (ETM+): 0.52~ 0.9		
Spatial Resolution	*30 m (Pan: 15m)*	*30m*	*120 m (ETM+7: 60m)*
Swath width	*185 km*		
Revisited Frequency	*16 days*		

Table 2: Specification of ASTER (Advanced Spaceborne Thermal Emission and Reflectance Radiometer) data

Acquired in Nov.2003			
Band number & wavelength (micro-meter)	**VNIR** (Visible & Near Infrared)	**SWIR** (Short Wave Infrared)	**TIR** (Thermal Infrared)
	Band 1 (Green): 0.52~0.60	*Band 4: 1.600~1.700*	*Band 10: 8.125~8.475*
	Band 2 (Red): 0.63~0.69	*Band 5: 2.145~2.185*	*Band 11: 8.475~8.825*
		Band 6: 2.185~2.225	*Band 12: 8.925~9.275*
		Band 7: 2.235~2.285	*Band 13: 10.25~10.95*
	Band 3N (NIR): 0.76~0.86	*Band 8: 2.295~2.365*	
		Band 9: 2.360~2.430	*Band 14: 10.95~11.65*
Spatial Resolution	*15m*	*30m*	*90m*
Swath width	*60 km*		
Revisited Frequency	*16 days*		

Method

Image pre-processing

Considering the available images of Thai Binh are of different acquisition dates and are acquired by different sensors (MSS, TM, +ETM and ASTER) the radiometric and geometric corrections are needed in pre-processing procedures. Data providers and all the Digital Numbers were already converted into reflectance values of 32 bits by Radiometric Calibration. Geometric Correction was carried out by polynomial model using UTM WGS 84 projection. The details of Ground Control Point GCP and Root Mean Square RMS are presented in the table 3.
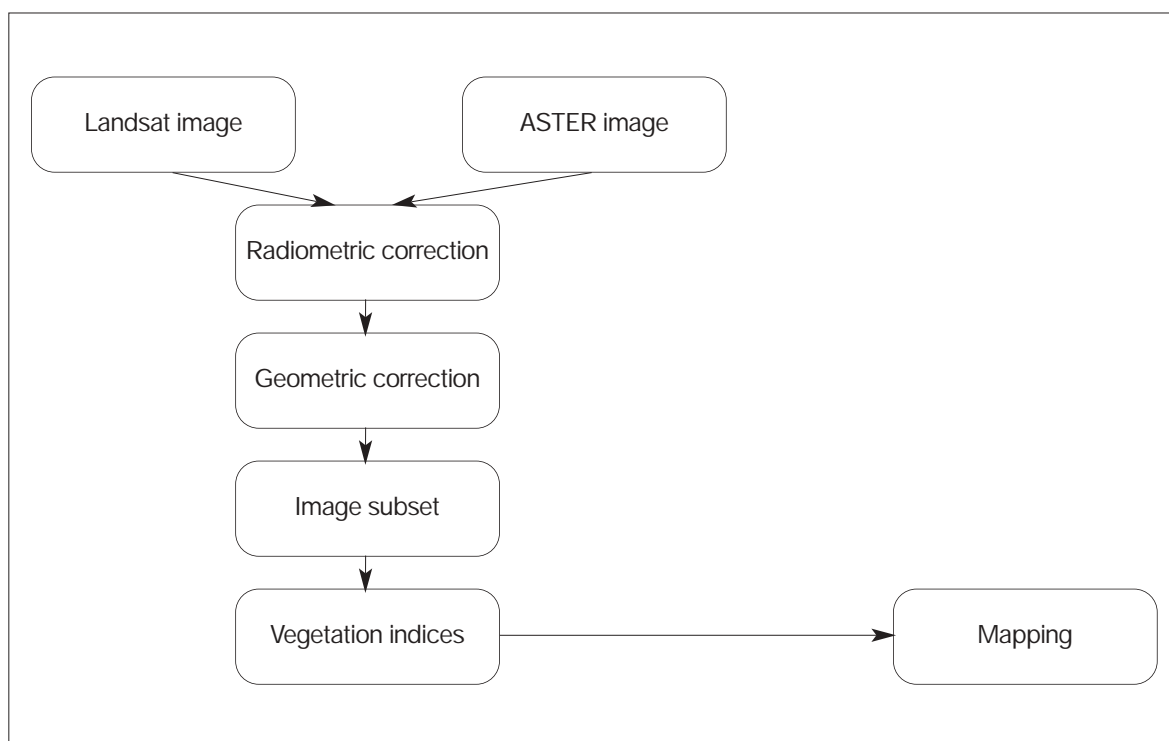
Figure 1: *Image Processing Flowchart*

Table 3: *GCP used for geometric correction of ASTER image 2003, 29 November scene 1*

ASTER image 2003, 29 November (scene 1) RMS Error: (0.29; 0.35)			
ID	**Uncorrected X**	**Uncorrected Y**	**Georeferenced X**	**Georeferenced Y**
1	4287.1875	804.9375	636520.625	2248851.875
2	2904.9375	1563.8125	614310.625	2240731.875
3	3902.3125	1515.4375	629209.375	2239180.625
4	3587.4375	121.6875	627693.125	2260571.875
5	2292.5625	236.4375	608236.875	2261784.375
6	3219.59375	914.84375	620444.375	2249639.375
7	3491.5625	1975.3125	622079.375	2233301.875
8	2202.34375	1178.59375	604769.375	2248030.625
9	2814.8125	784.5625	614729.375	2252489.375
10	4138.5625	2029.5625	631545.625	2231028.125
11	4634.03125	76.96875	643318.125	2258855.625
12	2072.3125	2055.1875	600855.625	2235323.125

Table 4: GCP used for geometric correction of ASTER image 2003, 29 November scene 2

ID	Uncorrected X	Uncorrected Y	Georeferenced X	Georeferenced Y
ASTER image 2003, 29 November (scene 2) RMS Error: (0.25; 0.28)				
1	3488.4375	2228.4375	634396.875	2288654.375
2	2429.1875	2806.0625	617391.875	2282468.125
3	4128.0625	3880.6875	640151.25	2262701.25
4	2139.6875	3861.9375	610714.375	2267474.375
5	2005.4375	2158.4375	612559.0625	2293037.187
6	4484.84375	2685.03125	648144.6875	2279624.063
7	3466.40625	3274.40625	631710.3125	2273184.063
8	2909.03125	4104.09375	621576.875	2262146.875
9	4404.5625	3158.9375	645885.9375	2272780.938
10	3744.09375	3915.34375	634380.9375	2263057.812

Table 5: GCP used for geometric correction of ASTER image 31 August 2002

ID	Uncorrected X	Uncorrected Y	Georeferenced X	Georeferenced Y
ASTER image 13 August 2002 RMS Error: 0.20; 0.31				
1	1915.28125	2578.40625	632406.875	2247664.375
2	481.3125	3408.4375	609350.625	2238390.625
3	3545.5625	106.4375	661860.625	2280903.125
4	731.15625	155.28125	619967.8125	2286165.313
5	3965.8125	1569.0625	665000.625	2258289.375
6	2655.0625	3431.6875	641588.125	2233423.125
7	490.6875	1791.4375	612916.875	2262390.625
8	2239.4375	1124.4375	640308.125	2268563.125
9	2022.1875	157.0625	639130.625	2283391.875
10	1326.9375	878.9375	627284.375	2274159.375
11	3791.9375	2505.5625	660423.125	2244756.875
12	1034.5625	2363.8125	619779.375	2252731.875
13	2699.5625	2023.1875	645225.625	2254240.625
14	3637.098388	647.855779	662071.875	2272668.125
15	1542.6875	3663.6875	624570.625	2232346.875

Table 6: GCP used for geometric correction of Landsat image +ETM November 2001

ID	Uncorrected X	Uncorrected Y	Georeferenced X	Georeferenced Y
Landsat image November 2001 RMS error: (0.34, 0.38)				
1	912.0625	1054.1875	641173.75	2263341.25
2	1646.9375	438.5625	662111.25	2280911.25
3	104.8125	299.9375	618146.25	2284841.25
4	811.375	289.375	638271.25	2285158.75
5	1733.5625	1321.5625	664588.75	2255743.75
6	467.4375	834.0625	628505.625	2269595.625
7	1371.3125	1584.6875	654289.375	2248229.375
8	1698.0625	959.4375	663594.375	2266059.375
9	1063.9375	510.1875	645489.375	2278854.375
10	416.3125	510.4375	627029.375	2278843.125
11	1328.3125	1054.9375	653038.75	2263318.75
12	448.9375	1152.9375	627991.25	2260541.25

Table 7: GCP used for geometric correction of Landsat image +ETM September 2001

Landsat September 2001 RMS error: (0.37, 0.58)				
ID	*Uncorrected X*	*Uncorrected Y*	*Georeferenced X*	*Georeferenced Y*
1	840.1875	1368.8125	639113.75	2254381.25
2	413.3125	372.8125	626908.75	2282751.25
3	913.3125	1053.4375	641172.5	2263347.5
4	976.625	235.875	642951.25	2286676.25
5	1765.4375	1060.6875	665473.125	2263166.875
6	95.625	337.625	617856.25	2283783.75
7	358.1875	857.6875	625373.75	2268961.25

Table 8: GCP used for geometric correction of Landsat image TM November 1989

Landsat image November 2001 RMS error: (0.34, 0.38)				
ID	*Uncorrected X*	*Uncorrected Y*	*Georeferenced X*	*Georeferenced Y*
1	1535.3125	723.5625	658914.375	2272774.375
2	869.625	1158.125	639928.75	2260398.75
3	551.3125	117.9375	630845.625	2290039.375
4	631.1875	1428.6875	633108.75	2252686.25
5	681.3125	733.1875	634552.1995	2272502.24
6	1473.3125	1597.6875	657145.625	2247836.875
7	1768.3125	983.3125	665553.75	2265378.75
8	426.3125	674.9375	627281.875	2274161.875
9	1244.8125	727.3125	650619.375	2272665.625
10	1127.6875	1158.5625	647295.625	2260375.625
11	1210.3125	296.6875	649641.875	2284950.625
12	440.8125	1151.6875	627696.25	2260571.25

Table 9: GCP used for geometric correction of Landsat image MSS December 1975

Landsat December 1975 RMS error: (0.41, 0.50)				
ID	*Uncorrected X*	*Uncorrected Y*	*Georeferenced X*	*Georeferenced Y*
1	857.875	1132.375	639605.625	2261036.875
2	636.625	701.875	633274.375	2273323.125
3	1153.625	556.625	647997.5	2277472.5
4	80.875	379.625	617393.75	2282466.25
5	1106.375	1288.125	646698.125	2256586.875
6	1745.625	898.875	664921.875	2267711.875
7	1213.875	923.375	649768.125	2267011.875

Index Computing

Vegetation index (VI) is one of the physical indices we can compute from the spectral bands of remote sensing image. The vegetation index VI is used in different applications such as canopy and biomass estimation, crop monitoring and drought monitoring etc. In the literature, other VI are cited and differ in terms of spectral bands and the algorithms and in terms of application (Rouse et al 1974; Colwell et Suits 1975;

Huete, 1988; Richardson and Wiegand 1977; Baret et al. 1989; Kaufman et Tanré, 1992 ; Qi et al 1994). The paragraphs bellow describe some of these indices used for our study.

SAVI (Soil Adjusted Vegetation Index) computes the ratio between red and near infrared spectral region with some added terms to adjust for different brightness of background soil (Huete, 1988). Due to paddy

harvested time ends in October, the result of SAVI images during November-December presents the situation of natural vegetation in the province. The SAVI image of September helps to understand the agricultural activities in details. The Normalized Differential Water Index (NDWI) estimates the situation of water in the province. The ratio between red and Short Wave Infrared (SWIR) spectral region clearly enhanced water bodies to the brighter pixels (CPM, 2003).

$$SAVI = \left[(\frac{\rho_{nir} - \rho_{red} + L}{\rho_{nir} + \rho_{red}}) \times (1+L) \right] + 1$$

Where: p is the reflectance, L~ 0.5

$$NDWI = \left[\frac{\rho_{red} - \rho_{swir}}{\rho_{red} + \rho_{swir}} \right] + 1$$

Bare Soil Index (BI) was also computed to identify difference between agriculture and none agriculture vegetation. The bare soil, fallow lands, and vegetation (with marked background response) are enhanced when using the BI index (Jamalabad and Abkar, 2004).

$$BI = \frac{(\rho_{swir} + \rho_{red}) - (\rho_{nir} + \rho_{blue})}{(\rho_{swir} + \rho_{red}) - (\rho_{nir} + \rho_{blue})} + 1$$

As for 2003, the non-vegetation objects are additionally extracted from Urban Index UI (Kawamura, M., S. Jayamamana and Y. Tsujiko 1997) to emphasize the vegetation presence and UI is very helpful to discriminate vegetation and non-vegetation land cover types. The UI is calculated as following:

$$UI = \frac{(\rho_{swir2} - \rho_{red})}{(\rho_{swir2} + \rho_{red})} + 1$$

For Landsat MSS, we compute p_{nir} from band 3 and p_{red} from band 2. For Landsat TM and ETM+, p_{nir} is computed from band 4, p_{red} from band 3, p_{swir} from band 5 and p_{swir2} from band 7, p_{blue} from band 1. For ASTER, p_{red}, p_{nir}, p_{swir}, p_{swir2} are taken from band 2, 3, band 4, band 5 respectively. All the equations above provide value ranges from -1 to +1. To avoid negative value in further analysis, we have added +1 in each

equation. Thus, the resulted images will have value between 0~2 where higher value show the existence of the environment parameters (i.e. high in SAVI shows high in vegetation, high in NDWI shows high in water). We compute also mean and standard deviation from each index at commune level to analyze the environmental situation with socio-economic condition at each commune.

Scaling problem and solution
As explained in previous sector of this report, due to the difference of acquisition dates and especially, to the spectral band difference, the VI values computed for ASTER images vary between 0.80131286 and 1.18813098 meanwhile the range of VI computed for Landsat images is in between 0.64208417 and 1.09550542. In order to compare these values we need to scale the ASTER VI values to fit the Landsat VI range using relative scaling method. This method is described by the formula:

$$N = n * \delta + \alpha$$

Where:

$$\delta = \frac{x_{max} - x_{min}}{X_{max} - X_{min}}$$

And

$$\alpha = \frac{X_{min}}{\delta} - x_{min}$$

Where:
N: Grey level value after calibration
n: Orginal grey level value to be calibrated
δ: Stretching co-efficient for the set of pixel to be calibrated
α: Shifted co-efficient for each pixel
X_{max} Maximum grey level value of pixels in the standard image
X_{min} Minimum grey level value of pixels in the standard image
x_{max}: Maximum grey level value of pixels in the dependent image
x_{min}: Minimum grey level value of pixels in the dependent image

In this study, we used the value extracted from the image Landsat ETM+7 acquired in November 2001 as the reference.

Results

Multidate statistical variations of indices

SAVI, BI, NDWI and UI indices were computed in multi-temporal Landsat images and ASTER images (see fig. 2.1 to 2.19). The multidate statistical variations of computed indices are used to analyze the environmental changes with respect to vegetation, agriculture, water and urban activities. The indices after calibration have produced relative results based on electromagnetic spectrum recorded in the images. The mean score and coefficient of standard deviation of each index were carefully evaluated at commune level. Standard deviation of mean helped to understand the distribution pattern of the objects in the land surface.

Principally, the SAVI appears brighter in healthy vegetation areas whereas BI seems brighter in bare land areas. The high NDWI corresponds to the areas with high water content. The variation of UI index indicates the different density of urban and built areas.

The SAVI index of 1975, 1989, 2001, 2003 represent the natural vegetation coverage in brighter areas. It is because of seasonal variance in agriculture practice. The high content of chlorophyll can be observed in paddy field in September. The paddy harvest is completed at the end of October. Therefore, harvested paddy fields on the images taken during November and December have a high bare soil index BI and appear in brighter pixels.

Some inconsistencies in distribution pattern of the mean of SAVI are observed in some communes. Decreasing trend of natural vegetation is observed in past three Bare soil index of 2001 is also getting lower as compared to year 1989. Mean distribution of the bare soil index seems more consistent as compared to SAVI mean. Comparison of BI with SAVI makes sense of conventional agriculture occupancy as well as practices. There are not so much fluctuations in distribution of objects in BI. Decreasing patterns in SAVI and BI exposed the decreasing of conventional agriculture practices (i.e. paddy).

The result of NDWI is quite different than SAVI and BI. Increasing pattern is observed in water bodies although inconsistency in distribution of the water bodies is found in some communes.

Several farmers in the province are changing their traditional agriculture land to modern aquatic practices. It is one of the major factors that increased the water properties and reduced the vegetation properties as compared to 1980s. Direct relation of fish farms to the pig production was observed during the field visit. Pig waste is being used as a source of input for aquatic farming fertilization of ponds, nutrient for fishes. Thanks to the high demand of lean pork meat in the growing cities and flexible government policies, farmers are attracted to the integrated agriculture practices (pig and fish ponds).

There is very good compromise between water and urban index. Most of the urban areas are observed along the water bodies like rivers, canals and lakes. The increased urban activities in the province do not have significant impact in reducing water properties. But it has significant impact in reducing the vegetation. The UI mean increased as a peak in some communes whereas the SAVI mean decreased just like a gorge in the corresponding communes. So, the land of agriculture is being occupied by urban function. The conversion of agriculture land to urban uses is natural economic process in widely observed in Thai Binh.

Relation between vegetation activities and urban function was checked in September 2001 results and found correlation coefficient at -0.606. It has strong negative linear relation between the UI and SAVI mean, which suggest the urban activities replacing the natural environment significantly.

Vegetation is thus getting sparse day by day because of growing urban activities, integrated agriculture practices, government priorities on intensification of pig production and aquatic products.
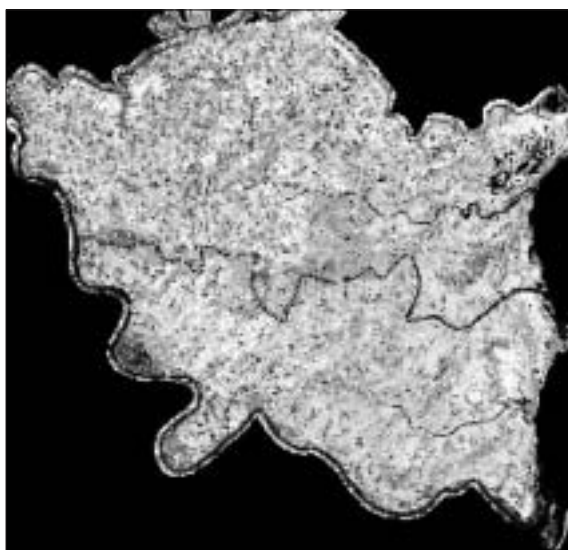
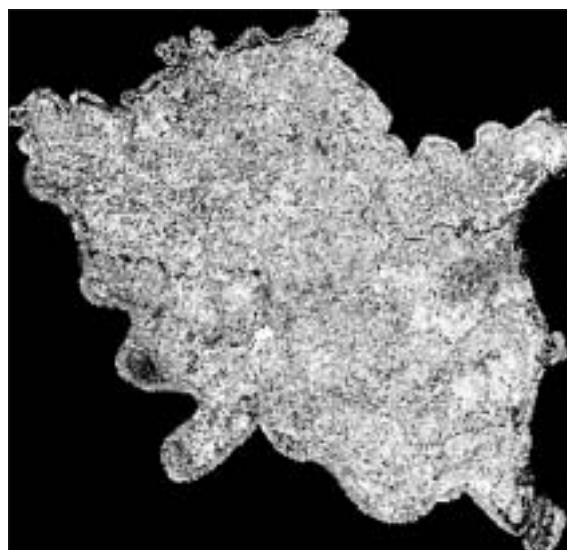*Figure 2.1: Bare soil index in 1989*
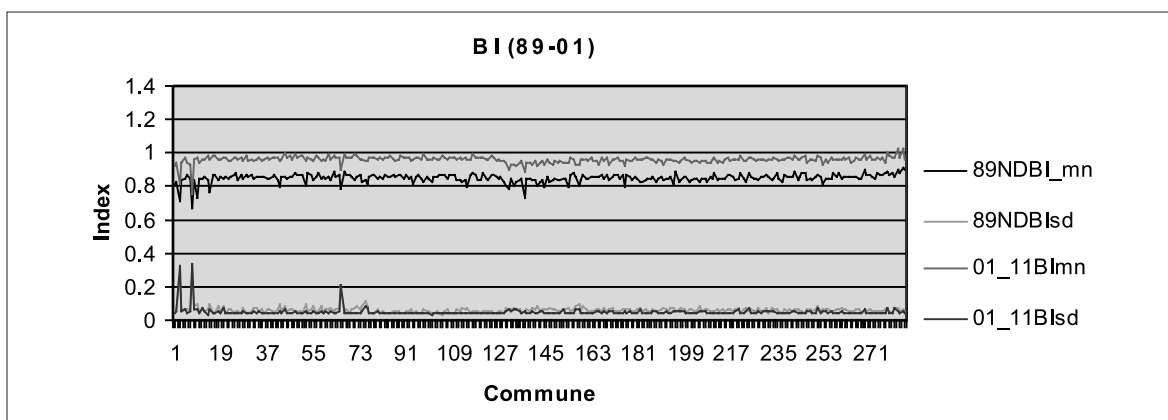

Figure 2.2: Bare soil index in 2001

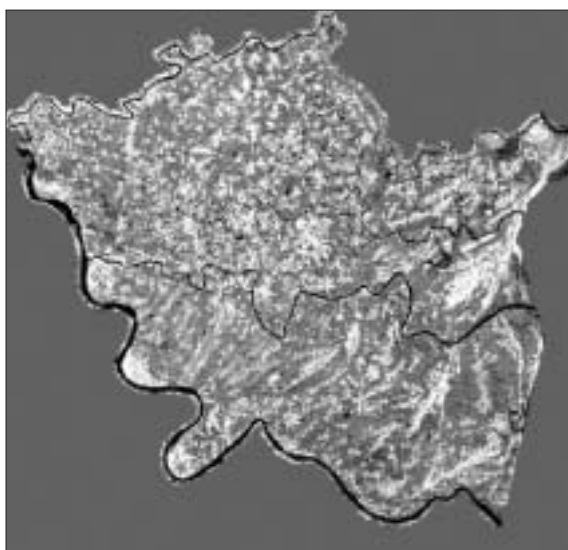*Figure 2.3: Bare soil index from 1989 and 2001 (mn – mean, sd- standard deviation)*
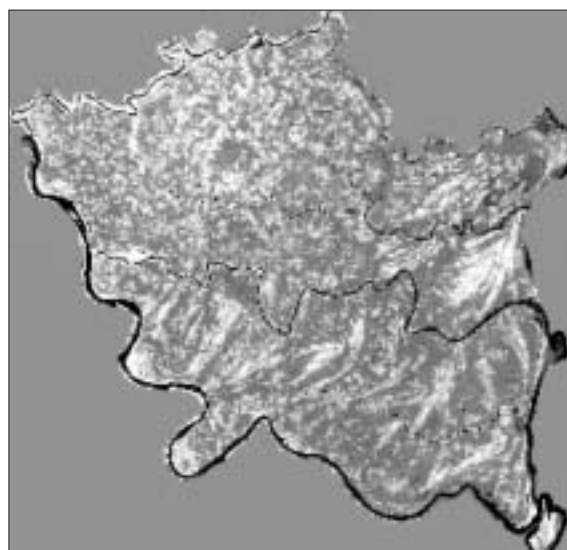

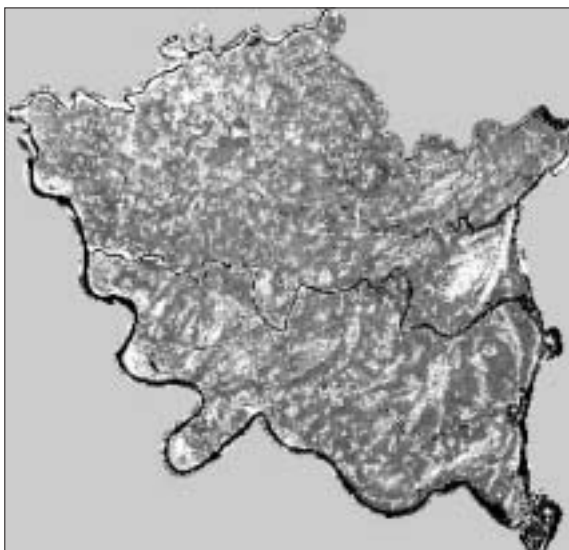*Figure 2.4: SAVI in December 1975*

Figure 2.5: SAVI in November 1989
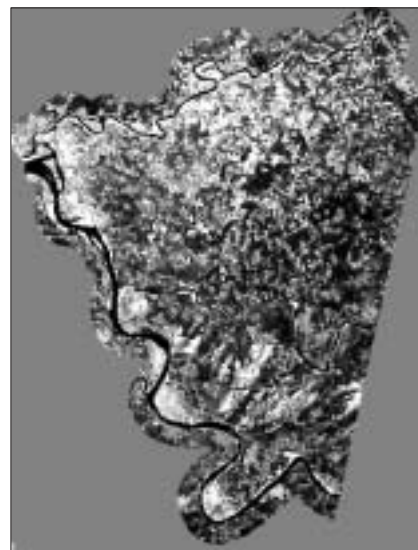
45

Figure 2.6: SAVI in 2001, November
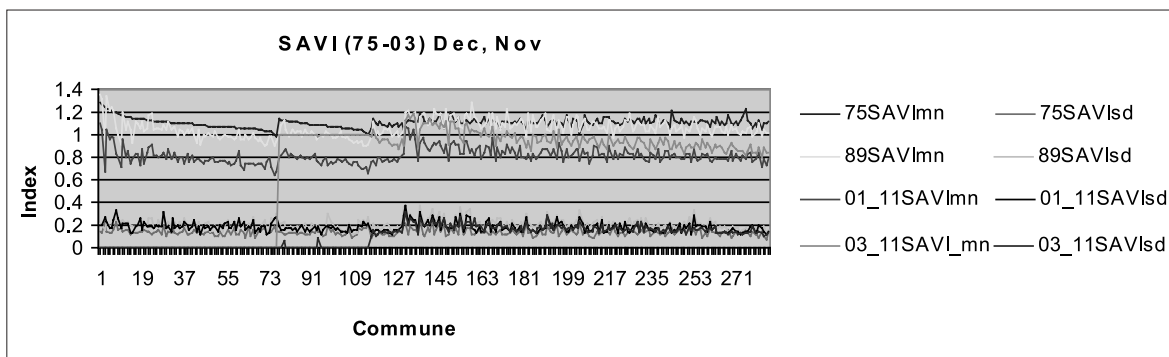

Figure 2.7: SAVI in November 2003

Figure 2.8: SAVI from Landsat image (1975 – 2001) and ASTER image (2003) at harvested season. Zero value is considered for communes from 1 to 116 due to the lack of image (mn- mean, sd-standard deviation)
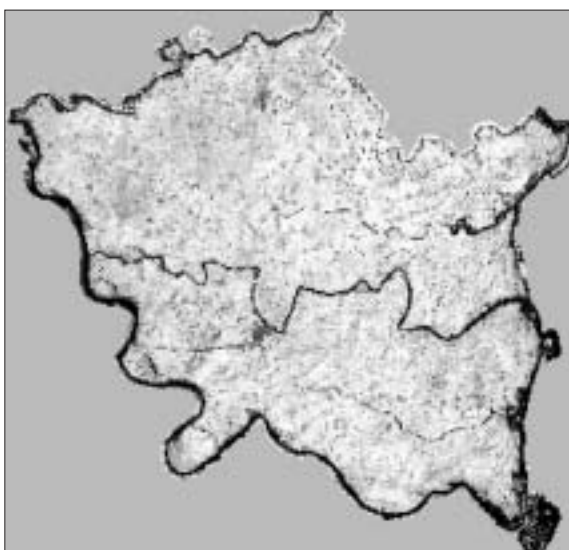
Figure 2.9: SAVI in September, 2001
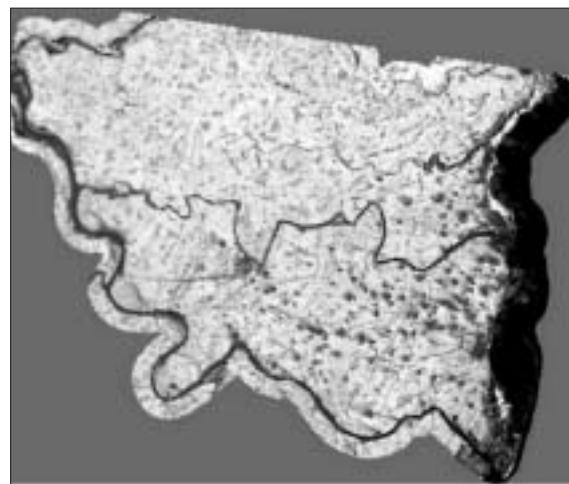
Figure 2.10: SAVI in August, 2002
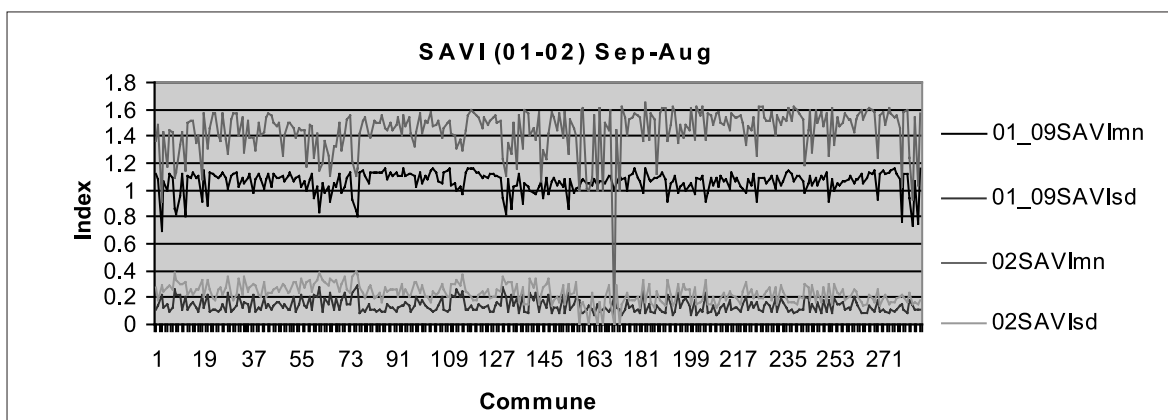
Figure 2.11: SAVI in farming season taken from Landsat image and ASTER image. The SAVI values from ASTER image are particularly high due to influence of cloud (mn- mean, sd- standard deviation)
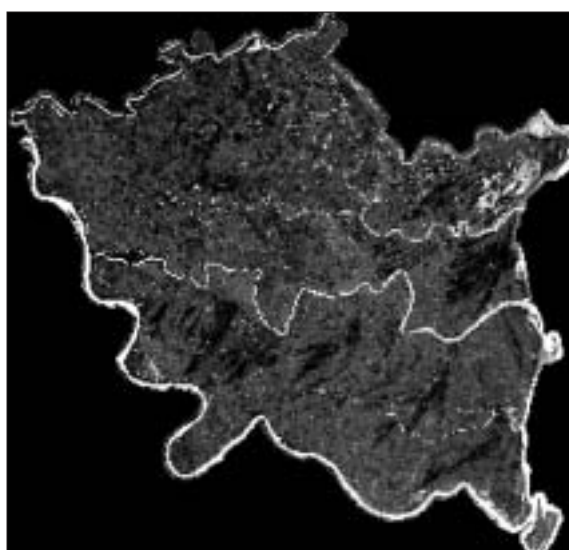
Figure 2.12: NDWI in November 1989
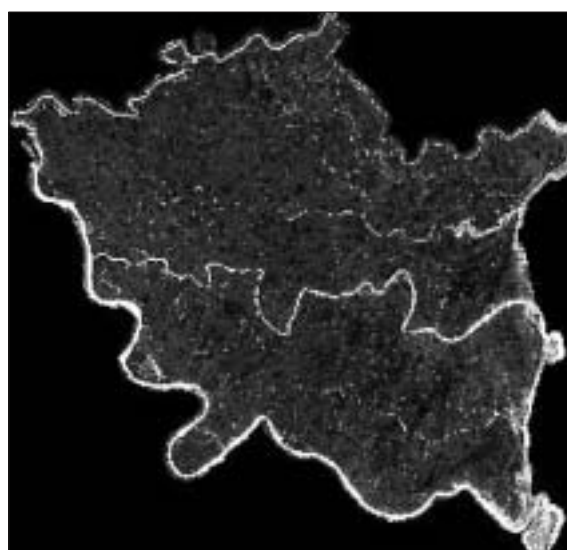
Figure 2.13: NDWI in 2001, September
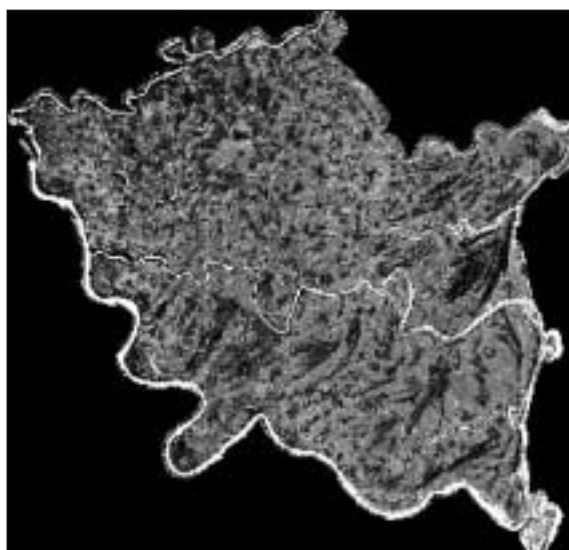
Figure 2.14: NDWI in 2001, November

Figure 2.15: NDWI in November 2003
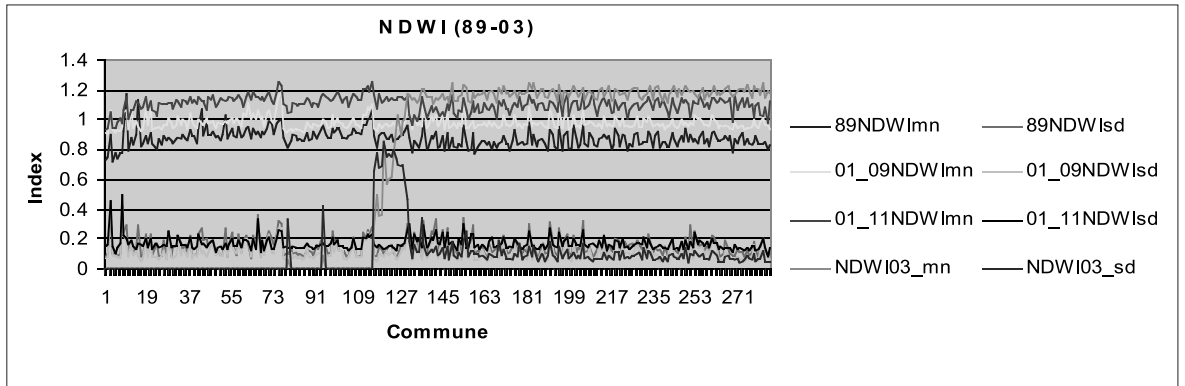
Figure 2.16: *NDWI from 1989 to 2003. NDWI from 2003 is considered 0 for 1st -116th ordered communes owing to the lack of image covering them (mn-mean, sd- standard deviation)*
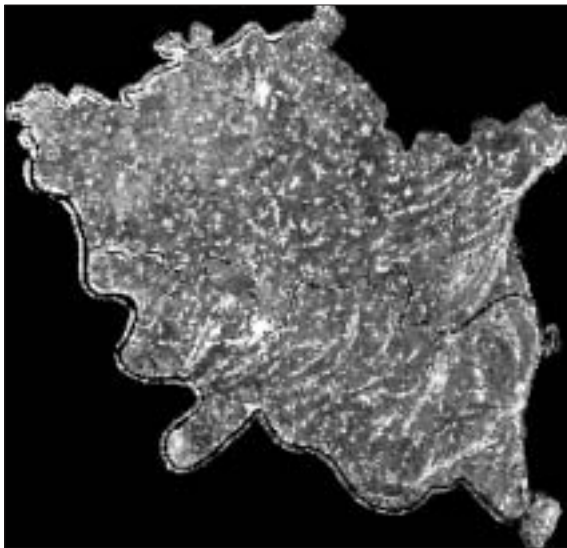
Figure 2.17: *UI from Landsat 2001, September*
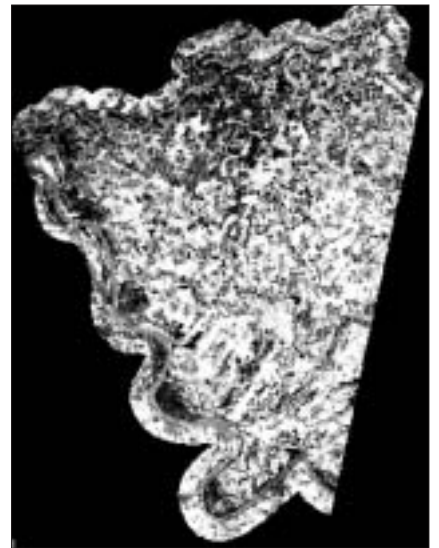
Figure 2.18: *UI from ASTER 2003, November*
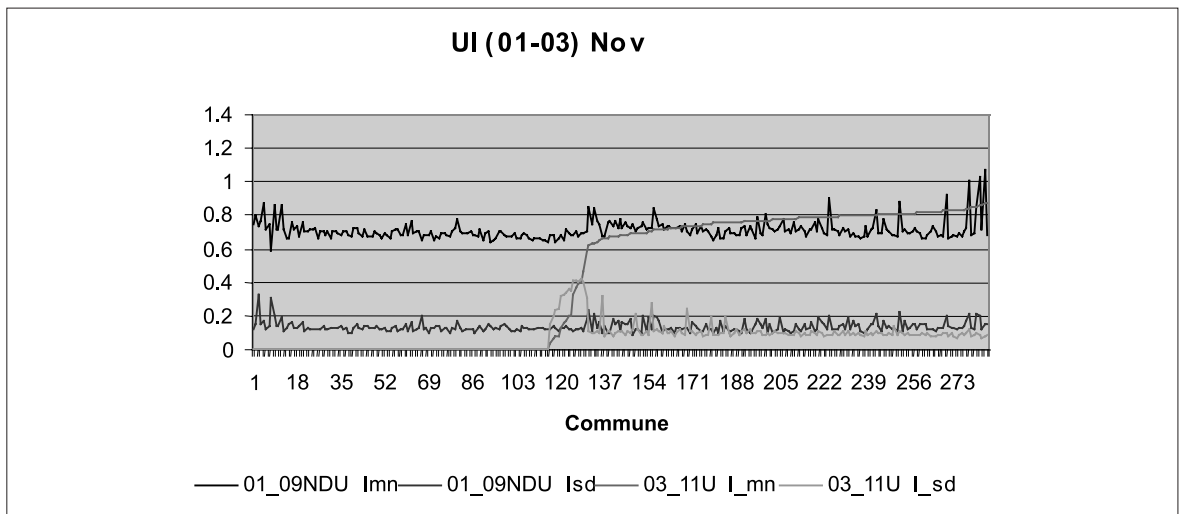
Figure 2.19: *UI from 2001 to 2003 (mn- mean, sd- standard deviation)*

Cartographic Representation of results

Due to the limits in statistic data, we cannot make a full representation of all physical index. The geo-referenced index images are crossed with the administrative map of Thai Binh to produce the normalized biophysical indices map at communal level, i.e., each commune of Thai Binh is now characterized by a series of Vegetation Index. The results are presented in a cartographic database of which the attribute data describing the computed indices are organized in relational model and very easy to manipulate in GIS environment.

Mean SAVI (Soil Adjusted Vegetation Index) Map by Commune

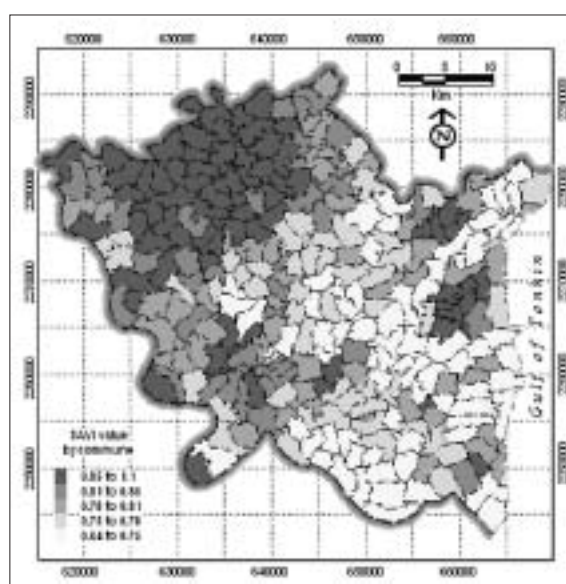*Figure 3.1: SAVI in December 1975*

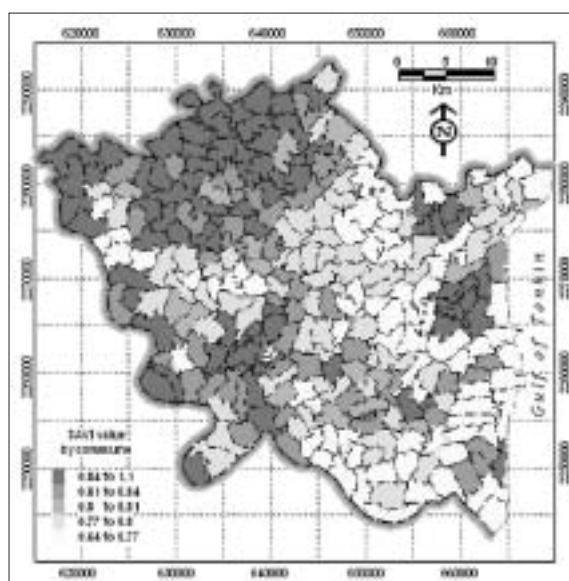*Figure 3.2: SAVI in November 1989*
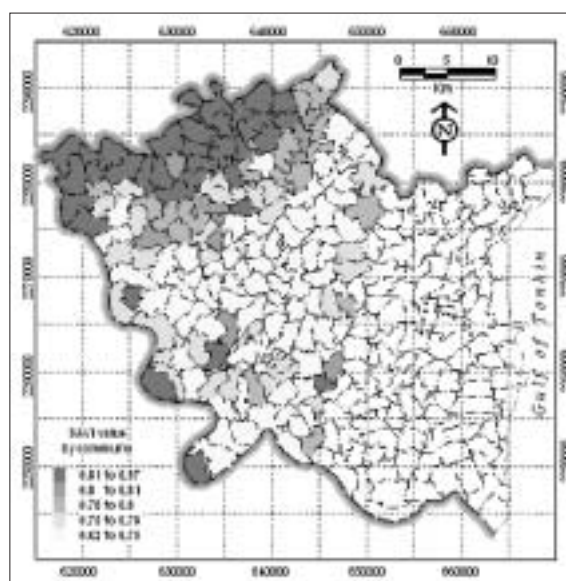

Figure 3.3: SAVI in November, 2001

Figure 3.4: SAVI in 2003

The SAVIs are extracted from Landsat and ASTER data, which were acquired during the harvesting season (Novembers). To facilitate the analysis, the SAVI mean values are associated to each commune and this value represents mean SAVI of the whole communal territory. As mentioned above, the scaling of SAVI values of the two dates of Landsat and ASTER data allows comparisons each with other. The higher communal SAVI the larger vegetation cover is (fig. 3). Due to its scene limitation, ASTER data covers only a part of Thai Binh and no value is computed for the non-data area.

As the Landsat and ASTER data are acquired in the period of similar climate conditions the atmospheric influence is negligible. The very low value of SAVI extracted from MSS data can be explained by its low spatial resolution (57m*79m) and bandwidths.

For the period from 1989 to 2003, the high SAVI values are concentrated in the Western and North West communes of Thai Binh even if the acquisition dates coincided to the harvest period. This phenomena may be explained by the presence of other cultures than rice in this period (for example vegetable, soya-bean etc.) which have been planted just after the harvest. To check this hypothesis, we used the statistic data on communal fertilizer consummation for winter plants and have found the high correlation between the consumption/use of fertilizer and SAVI values in these communes (Fig.4).
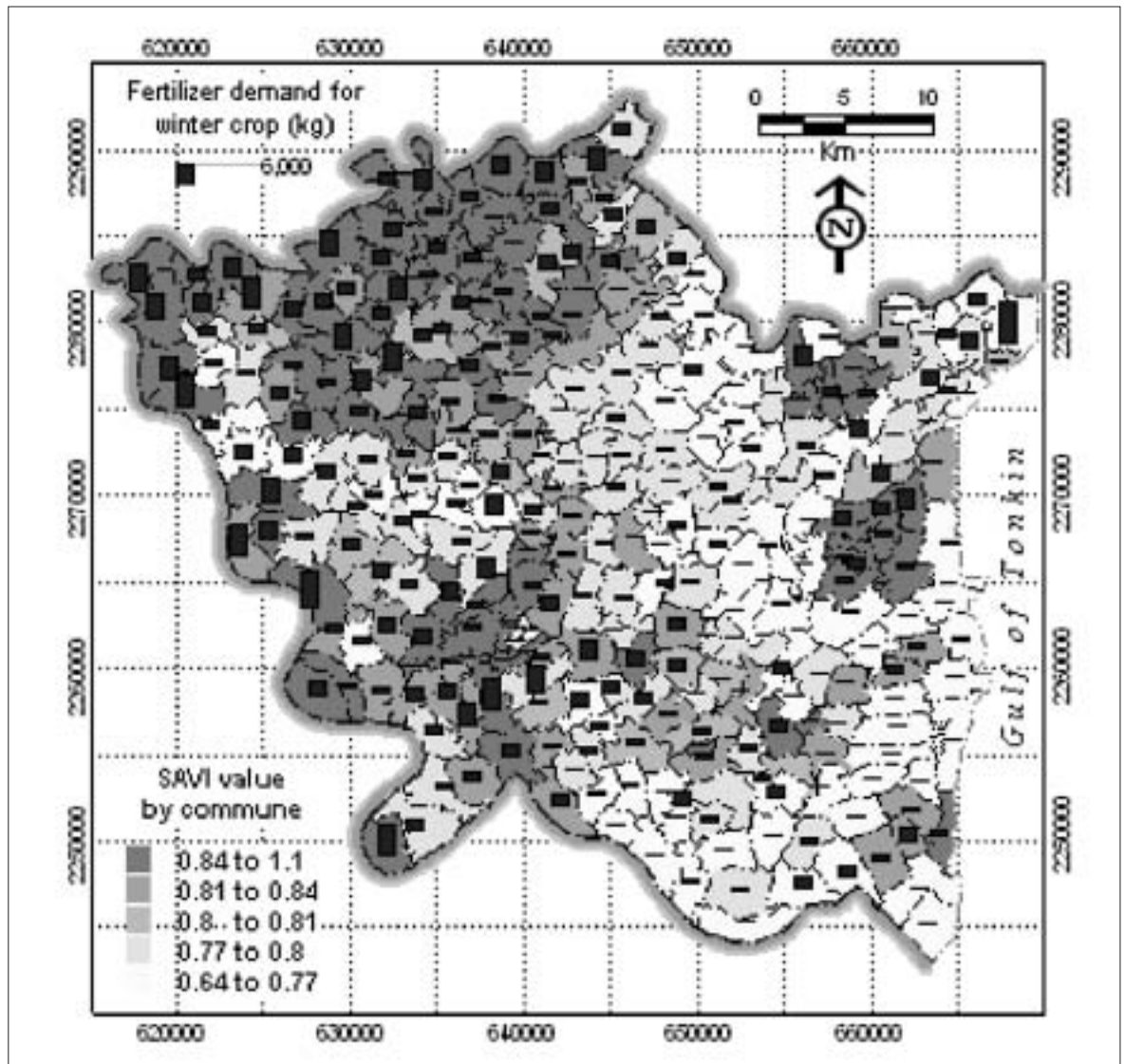

Figure 4: Correlation of fertilizer consumption and high SAVI values in West and North West Communes

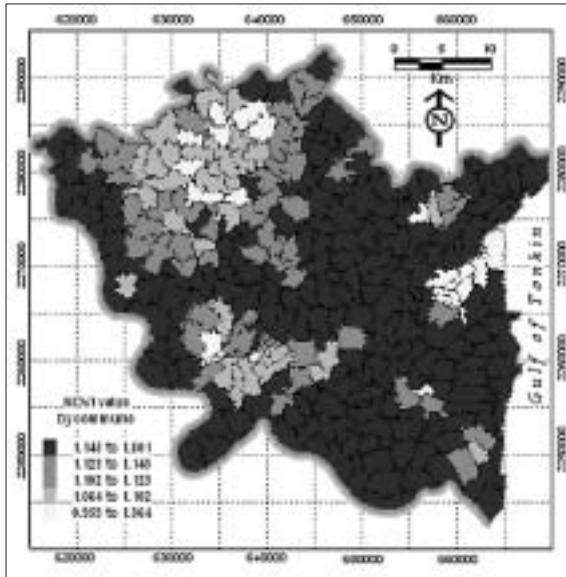**Mean NDWI (Normalized Difference Water Index) Map by Commune**

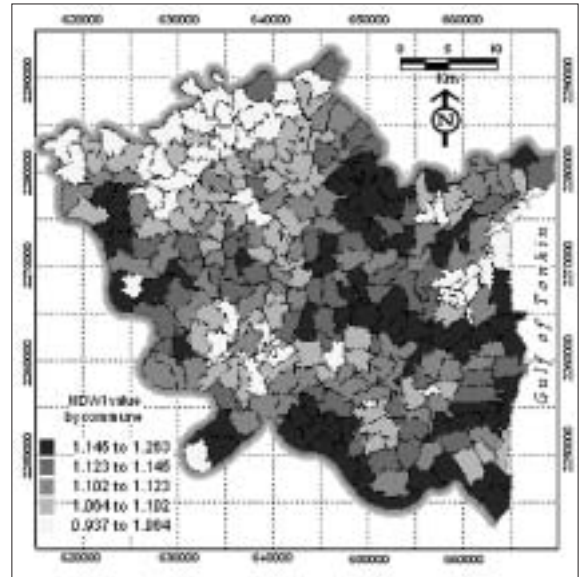*Figure 5.1: NDWI in November 1989*

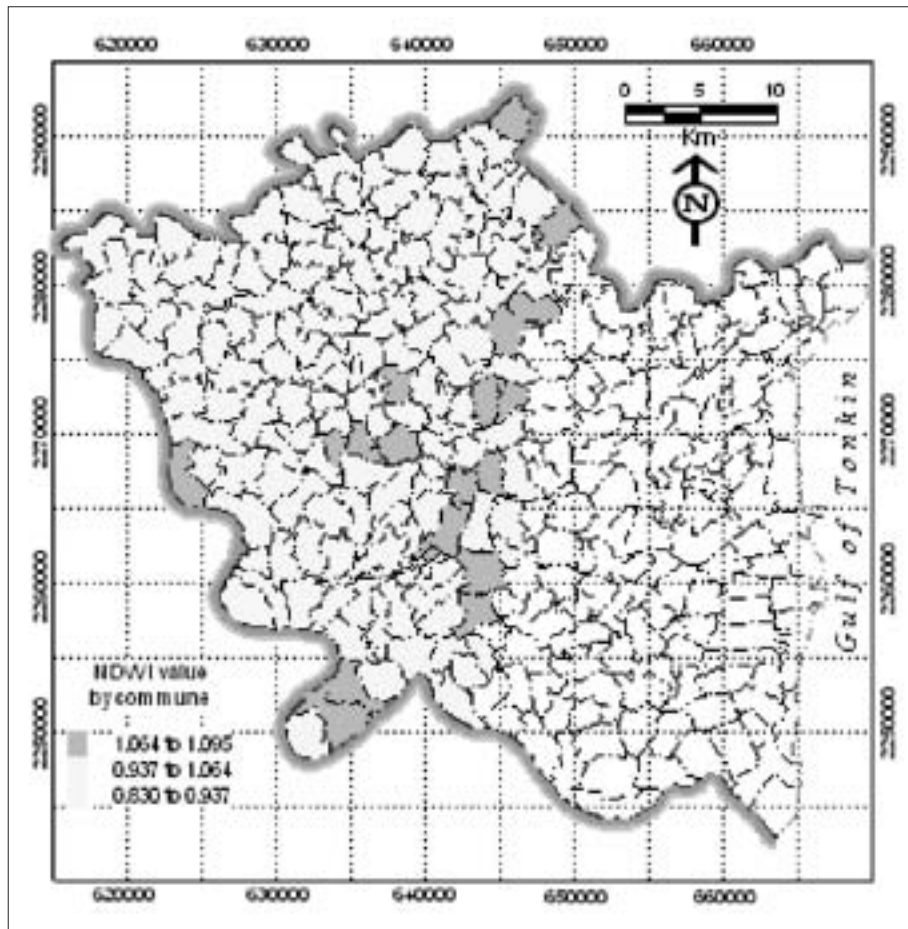*Figure 5.2: NDWI in November, 2001*

Figure 5.3: NDWI in November, 2001

NDWI was introduced by Gao (1996) to assess water content in a normalized way. This index increases with vegetation water content or from dry soil to free water. For the reference, we take the Land Use Map of 2000, the closest to Landsat image acquisition date we can have. The low NDWI values extracted from the Landsat TM and +ETM images acquired during dry season (November) of 1989 and 2001 indicate the low water content in soil and vegetation in the North West sector of the province. However, there observed a big difference in NDWI in the rest of territory in these two dates (Fig. 5.2, 5.3). This difference is thought related to the change of land use from rice in 1989 to Winter Crop in 2001.

The NDWI computed for ASTER image (Fig. 5.3) captured in November 2003 that covers only the West part of Thai Binh are low and corresponds to the area of Winter Crop.

In general, the NDWI values of North West Communes are lower than in other places (fig. 5.1 to 5.3) and showing the dryer soil conditions. In spite of that, their SAVI values indicate the existence of some vegetation (fig. 3.1 to 3.4) supposed to be winter vegetables as shown in Land Use Map (fig.7). These communes are mainly characterized by a high topography (see Chapter 2) and poorly irrigated terrain. Figure 6 shows the coincidence of winter crop and permanent vegetation (presented in black) with the areas of low NDWI values (between 0.937 and 1.102).
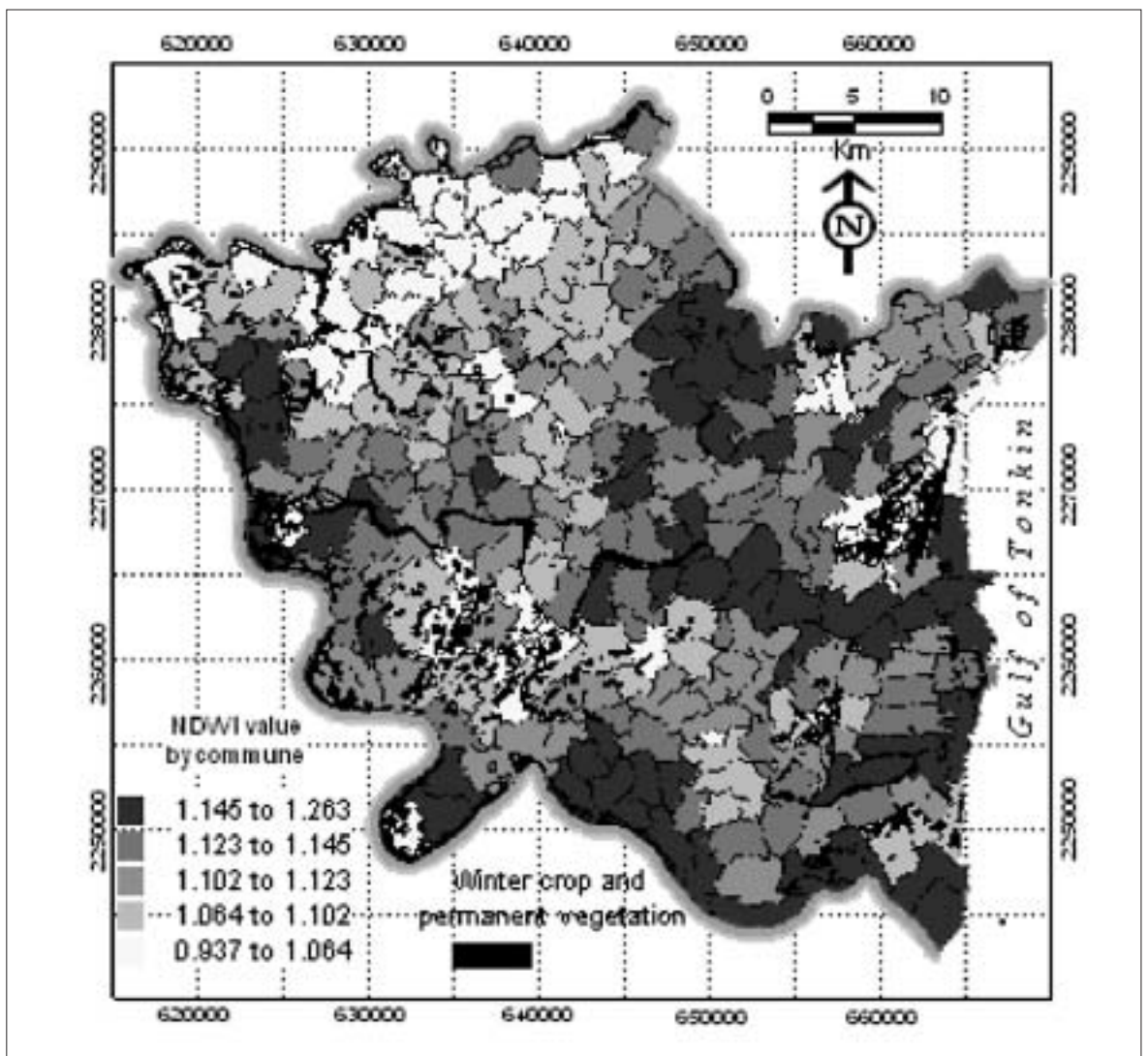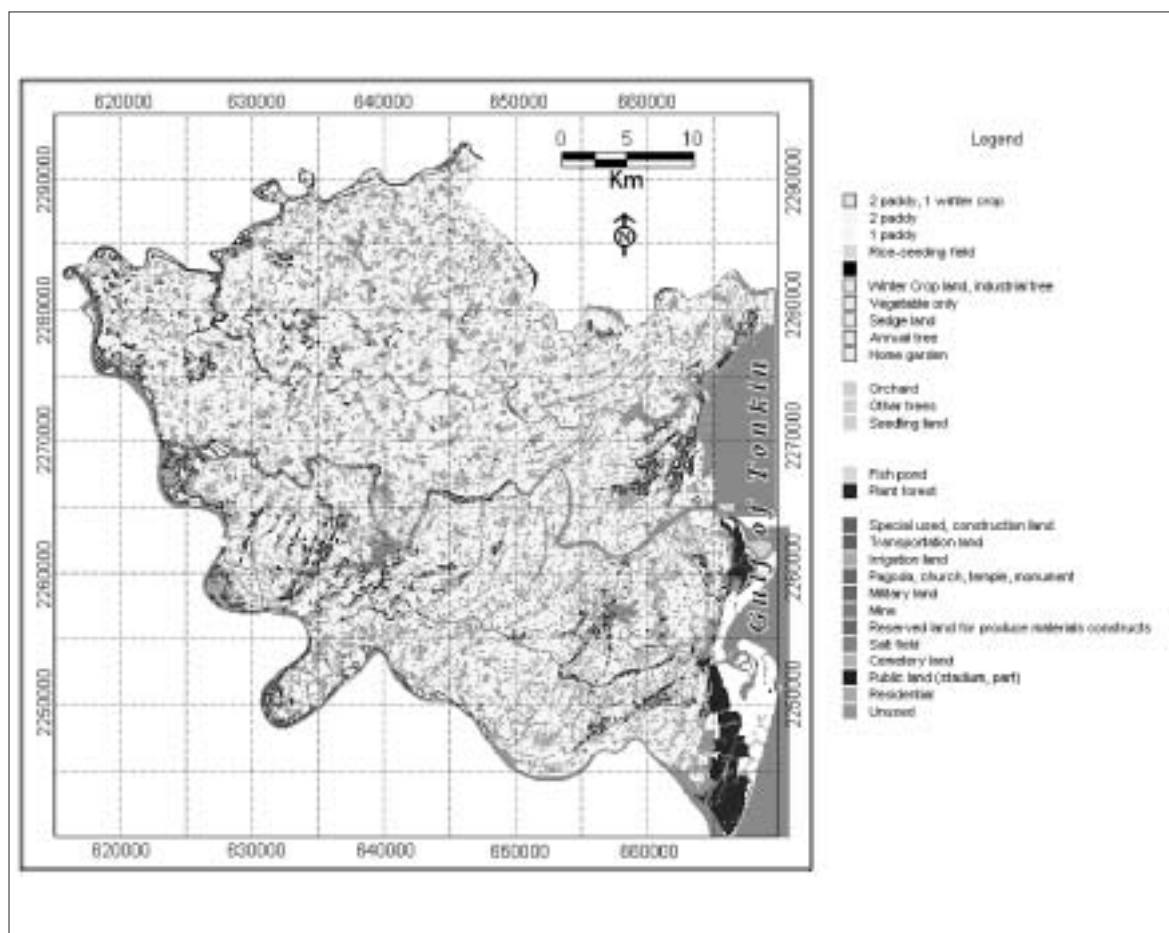

Figure 6: NDWI in November, 2001

Figure 6: Land use map of Thai Binh 2000 (Source Thai Binh Province)

Conclusion

Different physical indices extracted from a time series of satellite images between 1975 and 2003 allow characterizing the changes of land cover in Thai Binh in this period. Based on SAVI, UI and BI indices change evaluation, the surface of winter crop appeared to decrease gradually and concentrate mainly in suburb communes of Thai Binh City and the adjacent communes of Vu Thu and Dong Hung Districts.

The communes having high NDWI (1.102~1.263) have been reduced in the period 1989-2003. The brutal decrease of NDWI scale computed for ASTER image have highlighted the difference in spatial and spectral resolution of this sensor; this is to be verified by ancillary statistic data.

Comparison between SAVI and NDWI values evaluated the spatial repartition of dry season land cover types; where the high SAVI values (0.8-1.1) coincide with low values of NDWI (0.937-1.102), we can observe the presence of winter crop. This inverse relation could be used to monitor the winter crop in dry season.

For the first time, we have found a good correlation between fertilizer demand statistics and high values of SAVI which indicate the high demand in fertilizer of North West communes where the winter crop are predominant in dry season.

The integration of SAVI, NDWI, UI and BI on the administrative map with communal boundaries of Thai Binh provides a good tool for spatial analysis of multi-temporal changes of land cover characteristics and for analyzing spatial correlation between these characteristics and other socio-economic data we may have in Thai Binh

References

1. Arbelo Rodríguez, C.D., A. Rodríguez Rodríguez, J.A. Guerra García and J.L. Mora Hernández, (2002), Soil Quality and Plant Succession in Forest Andosols, 12th ISCO Conference, Beijing, pp 452- 458.

2. Baret F.G., G. Guyot and D.-J. Major, 1989. A vegetation index which minimizes soil brightness effects on LAI and APAR estimation, 12th Canadian Symposium on Remote Sensing, Canadian Remote Sensing Society, Vancouver, p. 1355-1358.

3. Barnes, E.W., K.A. Sudduth, J.W. Hummel, S.M. Lesch, D.L. Corwin, C. Yang, C.S.T. Daughtry and W.C. Bausch (2003). Remote- and ground-based sensor techniques to map soil properties. Photogrammetric Engineering and Remote Sensing 69 619-630.

4. Colwell G.E. and G.H. Suits, 1975. Yield prediction by analysis of multispectral scanner data, NASA-CR 141865, ERlm 109600-17-F, NASA.

5. Huete, A.R., 1988. Asoil –adjusted vegetation index (SAVI), Remote Sensing of Environment, no 25, p.295-309.

6. Jamalabad, M. S. and A.A. Abkar (2004). Forest Canopy Density Monitoring, Using Satellite Images. XXth ISPRS Congress, Istanbul 12-23 July.

7. Kaufman, Y.-J. and D.-C. Tanré, 1992. Atmospherically Resistant Vegetation Index (ARVI) for EOS-MODIS, IEEE Transaction on Geoscience and Remote Sensing, vol. 30, no 2, p.261-270.

8. Kawamura, M., S. Jayamamana and Y. Tsujiko (1997). 'Comparison of Urbanization and Environmental Condition in Asian Cities using Satellite Remote Sensing Data'. Available online: http://www.gisdevelopment.net/aars/acrs/1997/ps1/ps2008.shtml [Downloaded: 12 January, 2006]

9. C. López-Fand, M.T. Pard, 2002, The impact of tillage systems and machinary traffic on some soil properties and crop yield in a calcic luvisol of central Spain, 12th ISCO Conference, Beijing, pp138-143.

10. Lunetta R.S. and C.D.Elvidge, (Editors), 1998, Remote Sensing Change Detection: Environmental Monitoring Methods and Applications, Ann Arbor Press, Michigan, 318 p.

11. Palacios-Orueta, A., J. E. Pinzon, D. A. Roberts, and S. L. Ustin. (1998). "emote sensing of soil properties in the Santa Monica Mountains: Hierarchical Foreground and Background Analysis." Seventh Annual JPL Airborne Earth Science Workshop, Pasadena, CA. January 12-16, 1998.

12. Qi J., A. Chenbouni, A.R. Huete, Y.H. Kerr and S. Soroonshian, 1994. A Modified Soil Adjusted Vegetation Index (MSAVI), Remote Sensing of Environement, no 48, p. 119-126.

13. Richardson, A. and C. Wiegand, 1977. Distinguishing vegetation from soil background information, Photogrametric Engineering and Remote Sensing. No 43, p.1522-1541.

14. Rouse, J.W., R.H. Haas, J.A. Schell, D.W. Deering and J.C. Harla, 1974. Monitoring the vernal advancement retrogradation (Green Wave Effect) of natural vegetation, Maryland, USANASA/GFSC, Greenbelt.

15. Smith, W.N., Desjardins, R.L., Grant, B. and Lemke, R., 2002, Estimated N2O Emissions as Influenced by Agricultural Practices in Canada, 12th ISCO Conference, Beijing 2002, pp 317- 323.

16. Uno, Y., Prasher, S.O., Patel, R.M., Strachan, I.B. and Pattey, E. 2005. Development of field-scale soil organic matter content estimation models in Eastern Canada using airborne hyperspectral imagery. Canadian Biosystems Engineering/Le génie des biosystèmes au Canada 47: 1.9 - 1.14